FIRE PERFORMANCE OF PARTITION ASSEMBLIES*

Samuel L. Manzello†, Richard G. Gann, Scott R. Kukuck,
Kuldeep Prasad, and Walter W. Jones
Building and Fire Research Laboratory
National Institute of Standards and Technology
Gaithersburg, MD 20899-8662 USA

ABSTRACT

A series of real-scale compartment tests were performed to provide information on the phenomenology of partition response, and failure, to guide model development. Two wall assemblies of 2.44 m x 2.44 m were exposed to two intense fires from the time of ignition to beyond flashover. The assemblies were constructed using type X gypsum panels. The stud spacing and stud dimensions were fixed for both assemblies. Heat flux gauges provided time histories of the energy incident on the walls, while thermocouples provided data on the propagation of heat through the walls and on the progress toward perforation. Visual and infrared cameras were used to image partition behavior during the fire exposure. Results obtained from these experiments is presented and discussed.

INTRODUCTION

For nearly a century, the cornerstone of fire safety in buildings has been the ability to confine a fire for a time sufficient to allow successful evacuation of the occupants. To effect this, the partitions in a building (walls, floors, ceilings) are rated based on their resistance to the passage of heat and smoke. In the U.S., the standard test method for determining these ratings is ASTM E119[1], first published in 1918 and updated periodically by ASTM Committee E5, Fire Standards. A similar international standard is ISO 834[2], which is maintained by ISO TC92 SC2, Fire Containment. Rating requirements are then used in a prescriptive manner, based on the use and location of building elements within a structure. Use of these standards has been successful in reducing the number of fires that have caused loss of life and property.

Compartmentation is especially important in tall buildings, because egress of numerous occupants can be a complex and time-consuming process. Intact barriers prevent the spread of flame, keep the egress paths available, and increase the safe time in places of refuge. For all these functions, it is necessary to know, in terms of real time, how long the interior partitions in a building will contain flames and smoke.

There are three means by which a failure of a non-combustible partition (*i.e.*, wall) can increase the hazard from a building fire and there are three correlated failure modes of the wall listed in Table I. One means of obtaining information regarding these failure modes could be through the use of large-scale furnace testing, as in ASTM E119[1] or ISO 834[2]. Large scale furnace testing is appropriate since it tests a large section of the actual wall. The use of

† Corresponding Author, samuel.manzello@nist.gov, Office: +1-301-975-6891 Fax: +1-301-975-4052

large sections is important, since partitions are not normally simple one-dimensional constructs. Unfortunately, it has long been known that current fire resistance ratings obtained in furnaces do not coincide with actual safety times, but rather only provide *relative* guidance[1-2]. Thus, a two-hour rated partition may not contain an actual fire for two hours, but is likely to contain heat and smoke longer than a one-hour partition. Both the absolute values and the differences between ratings depend on the nature of the fire and the composition of the particular partition[3-6].

Table 1. Relation Between Partition Failure and Increased Hazard

Hazard	Failure Characteristic
Thermal ignition of combustibles beyond current fire compartment	Excessive temperature on reverse side of wall
Spread of fire effluent beyond current fire compartment	Cracks or openings through wall
Spread of flames beyond current fire compartment	Opening in wall

Many investigators have recognized the importance of modeling the response of both wood and steel framed partition assemblies to fire exposure[7-13]. Such models can generally only predict the behavior of the partition up to the point of the thermal insulation criterion (row 1 in Table 1), as specified under ASTM E119[1] and ISO 834[2]. As mentioned, all failures modes are needed to provide an absolute time for how long a partition can contain flames and smoke.

We have embarked on a course to provide a methodology for inclusion in performance-based design of buildings. The research involves obtaining real-scale experimental data, modeling the behavior of partitions as they are driven to failure by the fire, and developing recommendations for obtaining input parameters from modifications to standard fire resistance tests such as ASTM E119[1] and ISO 834[2].

This paper presents the preliminary results of such real-scale compartment tests performed to provide information on the phenomenology of partition response and failure and also quantitative information to guide the model development. It is important to note that these tests were conducted under actual fire conditions rather than in a furnace. The type of partition assembly considered was non-load bearing walls of gypsum panels attached with screws to steel studs. This type of construction was selected since it is the most common interior construction in tall buildings.

EXPERIMENTAL DESCRIPTION

Two types of non-load bearing walls consisting of gypsum panels attached to steel studs were used. The exposed face construction was the same for both assemblies; differences in construction occurred at the unexposed face. The dimensions of each assembly were 2.44 m by 2.44 m. Steel studs (29 mm by 92 mm) were spaced at 609 mm and type X gypsum panels (USG Fire Code Core[‡]) with a thickness of 15.9 mm were attached vertically to the studs using type S drywall screws spaced at 305 mm. The joints were taped and spackled prior to fire initiation within the compartment. Walls were constructed under ASTM guidelines for non-load bearing wall assemblies[14-17].

[‡] Certain commercial products are identified to adequately describe the experimental procedure. This in no way implies endorsement from NIST.

Figure 1 (a) displays Assembly One, which consisted of two single (1.22 m by 2.44 m) gypsum panels installed on the exposed face. Assembly Two was similar to Assembly One except that a single (1.22 m by 2.44 m) gypsum panel was installed on the right side of the unexposed face (see figure 2 (a-b)). Assembly Two was constructed to investigate the influence of a cavity within the assembly on partition behavior under a fire load. Since only one side of assembly two was fitted with a gypsum panel on the unexposed face, it was imperative to seal the service holes in the studs to simulate the cavity that would be created if another gypsum panel were fitted to the left side of the assembly. To facilitate the explanation of partition behavior observed during the fire exposure, the space between the studs was designated as section 1 thru section 4 (see fig. 1 (a) and fig. 2 (a)).

Temperatures were obtained using type K thermocouples (22 gauge) attached to the gypsum panels. Temperatures were obtained at: (1) the exposed surface, (2) within the gypsum board cavity for the double layer assembly, and (3) on the unexposed face. They collectively provided input for understanding the thermal load imparted by the fire to the partition assembly and for gaining insights into the conditions for crack and opening production. Bare thermocouples were used both on the exposed face and within the gypsum board cavity. Thermocouples at the unexposed face were placed under insulating pads, as specified in ASTM E119[1] in order to compare these measurements to the failure modes of the standard test. To model the unexposed temperatures accurately, one must account for the thermal resistance induced by the pads[10].

Four Schmidt-Boelter water-cooled total heat flux gauges were used to measure the heat flux incident on the walls. The positions of all four gauges were the same for both wall assemblies tested and are shown in figure 3. Two gauges were mounted flush to one of the gypsum panels and two gauges were mounted flush to the column adjacent to the other vertically mounted gypsum panel. The gauges were mounted on the column in order to have one of the vertically mounted gypsum panels free from holes necessary for gauge mounting. For the gauges mounted on the gypsum panel, a custom bracket was constructed to support the weight of the gauges and water lines.

To mitigate water condensation on the gauge surface, each gauge was water cooled to 75 °C ± 5 °C, which is well above the dew point temperature. Since soot deposition on the gauge surface was not desired, each gauge was purged with N_2 for 3 s every 120 s, during the test. The purge signal was apparent and was removed from the temporal heat flux trace. Each gauge was provided with a calibration from the manufacturer. Nonetheless, the gauges were re-calibrated at NIST prior to the test series at 75 °C. The gauges were subsequently re-calibrated upon completion of the test series. The calibrations before and after the test series agreed to within the uncertainty of the calibration procedure.

The unexposed face of each partition assembly was imaged using a standard (visual) video camera with a framing rate of 30 frames/s. In addition, an infrared camera was used to image the unexposed face, also at 30 frames/s. In order to have the unexposed face fill the field of view of the IR camera, the IR camera had to be placed close to the assembly. Consequently, care was taken to avoid damage to the camera from the heat generated by the fire. This problem was circumvented with the standard video camera by fitting it with an appropriate zoom lens. Both infrared and standard video cameras were recorded on mini-digital video (mini-DV) cassettes for subsequent image analysis. Prior to each test, photographs were taken at 2048 x 1024 pixel resolution of both the exposed and unexposed face using a digital camera fitted with a zoom lens. Another series of photographs were taken of the exposed and unexposed face upon completion of each test.

The size of the compartment for the fire experiments was 11 m long by 7.3 m wide by 3.4 m high. A 2.44 m by 2.44 m opening was constructed on the lower 7.3 m side of the compartment so that each partition assembly could be switched out for each fire test. A

similar construction and mounting methodology was followed for both assemblies. First, the exposed face was attached to the steel studs. The entire assembly was mounted flush to the ceiling of the compartment and all instrumentation was installed while the partition assembly was mounted. After the fire was over, Assembly One was removed and the process was repeated for Assembly Two.

The compartment was constructed to simulate a typical office space that would be found in tall buildings. Accordingly, the combustibles within the compartment consisted of three workstations for each of the fire exposures reported here. The total burn time for each fire was approximately 45 minutes. Further details of the compartment and the combustibles within the compartment are available elsewhere[18].

RESULTS AND DISCUSSION

From pictures of Assembly One taken immediately after the fire test it was clear that the paper on the exposed face burned off and significant cracking occurred on both gypsum panels. This was consistent with the well known contracting of gypsum panels due to dehydration upon heating[10]. The cracks appeared along the seam between the two gypsum panels and at the screw locations. The formation of cracks at the screw locations was expected since it is at these locations that the greatest mechanical stress exists. In addition, a series of transverse cracks were observed to form in both gypsum panels.

The following is experimentally derived information on the sequencing that led to these failures in Assembly One:

1. From the videographic records, the paper on section 4 (far right - see figure 1 (a) of unexposed face) was the first to char. Subsequent to this, the paper began to char on section 3. Section 2 then charred and flaming was observed. The flame originated near the top, and propagated both upward and downward. The flames propagated towards the location of thermocouple 6. After this, flames were visible on the bottom of section 4 (near thermocouple location 10). The last area of extended flaming was observed on section 1. Flames started near thermocouple locations 8 and 12. The flame quickly propagated upwards and engulfed most of section 1.

2. From the individual IR and standard video frames, the temporal evolution of openings and crack propagation was observed to occur in the following order: (1) opening at joint between the two vertically mounted gypsum panels (t = 964 s); (2) cracks at the screw locations along studs (t = 1306 s); (3) transverse cracks (t = 1499 s, crack started in section 2, t = 1569 s, crack started at section 1). It is important to note that the transverse cracks that formed on the exposed face, corresponding to section 3 and section 4 on the unexposed face, were not visible on the unexposed face.

3. Plotted in figure 4 (a) are the exposed face temperature measurements. The combined uncertainty for the temperature measurements is ± 10 °C for temperatures less than 200 °C and ± 30 °C for temperatures larger than 200 °C. The temperatures at thermocouple 13 were higher than thermocouple 14. The same trend was observed for thermocouples 15 and 16. This was expected since thermocouples 13 and 15 were placed higher in the wall. It is interesting to observe that the temperature was the highest at thermocouple locations 13 and 14, suggesting a hotspot on this side of the wall. The rate of the initial temperature rise was also faster at thermocouple locations 13 and 14 as well.

4. Figure 4 (b) displays the temporal evolution of measured total heat flux as function of position. The combined uncertainty in the total heat flux measurements was ± 6 %. From figure 5 (b), the total heat flux increased most rapidly at location HF-1 and

reached a value of 160 kW / m^2 at a time of 550 s after ignition. The total heat flux was highest at locations HF-1 and HF-2. Ultimately, the maximum value of total heat flux occurred at nearly the same time after ignition (1050 s) at all locations and varied from 140 kW / m^2 – 160 kW / m^2.

5. The timeline of events from the video-graphic records agreed with the magnitude of the unexposed face temperature measurements. The area where the most severe flaming was observed produced the highest measured temperature. The upper portion of section one, where the temperature rise was the fastest, produced the lowest temperatures since no flaming was observed at these locations.

The following is experimentally derived information on the sequencing that led to these failures in Assembly Two:

1. The timeline of events from the video-graphic records agreed with the magnitude of the unexposed face temperature measurements. The area where the most severe flaming was observed produced the highest measured temperature. The upper portion of section one, where the temperature rise was the fastest, produced the lowest temperatures since no flaming was observed at these locations.

2. From the video-graphic records of Assembly Two, the paper on section 2 (see figure 2 (a) of unexposed face) was the first to char. Subsequent to this, the paper began to char on section 1. After charring started on section 1, the upper half of panel two began to flame, near thermocouple location 5. The flames spread downwards towards thermocouple location 6. After this, flames were visible on the top of section 1 (near thermocouple location 7 and 11).

3. Throughout the test, the unexposed face on the side of the partition with the two gypsum panels did not char or produce open flame. In fact, the unexposed face on this side was visibly unaffected by the fire exposure. As a result, the cracking that resulted inside the panel on this side was not visible in either the IR or standard video view.

4. For the single gypsum panel, crack propagation was clearly visible from the video-graphic records. The transverse cracks appeared in section 2 (t = 1494 s) and later in section 1 (t = 1708 s). It is interesting to note that the order of crack propagation was similar to Assembly One. The openings at the joints between the two vertically mounted gypsum panels and cracks at the screw locations along the studs were not visible in the video records for Assembly Two.

5. The exposed face temperature measurements are displayed in figure 5 (a). The thermocouples failed at locations 13 and 14 at 850 s and 1150 s, respectively, into the fire exposure. These failures are speculated to be due to extreme heating of thermocouple connections 13 and 14, which were located inside the gypsum cavity. Complete temperature traces were obtained at thermocouple locations 15 and 16. In spite of the thermocouple failures, significant data was obtained to provide a clear picture of the temperature rise on the unexposed surface. From the figure, the largest temperature rise occurred at location 13, followed by thermocouple location 14. Similar to the data obtained for assembly one, the hotspot within the wall was clearly on the gypsum panel fitted with thermocouples 13 and 14.

6. Total heat flux data collected during the fire exposure is displayed in figure 5 (b). At location HF-1, the total heat flux increased rapidly to a peak value of 190 kW / m^2 at a time of 800 s. At this location (HF-1), total heat flux was sustained at more than 150 kW / m^2 for over 500 s. At the other upper position, HF-3, the total heat flux was

30 % less than location HF-1. The total heat flux was similar in magnitude (130 kW / m^2) for the two lower positions, HF-2 and HF-4. Overall, the fire exposure was qualitatively similar to the exposure in which assembly two was subjected, namely the magnitude of the total heat flux was greatest at locations HF-1 and HF-3.

7. Figure 6 (a) displays interior temperature measurements on the inside of the exposed board. Figure 6 (b) shows interior temperature measurements on the inside of the unexposed board. In addition**,** figure 6 (b) shows temperatures obtained within the steel studs (25, 26). Some salient features are apparent from these figures. The temperature rose faster on the inside of the exposed board at all locations compared to those temperatures at the same height on the inside of the unexposed board. For example, a noticeable temperature increase was observed 30 s after ignition (locations 17, 18, 21, 22, 27, and 28). On the contrary, a temperature rise was not detected at locations 19, 20, 23, 24, 29, and 30 until 125 s after ignition. The magnitude of the temperature on the inside of the exposed board was higher than their counterparts on the inside of the unexposed board. For the temperatures measured on the inside of the unexposed board, the temperatures varied greatly. (See figure 6 (b).) For example, at location 19, the measured temperature was 460 °C whereas at location 20, the measured temperature was 300 °C. As mentioned previously, it was not possible to see into the cavity during the fire test. Accordingly, to understand this difference in measured temperature, this panel was removed after the fire test. Upon inspection of the inside of the unexposed board, the paper was slightly brown near location 20, confirming that the paper did not burn at this location, which explained the lower temperature.

8. The outside face temperatures of the unexposed board are displayed in figure 7. The temperature rise on the outside face of the unexposed board was minimal. In fact, the temperatures rise was insufficient to result in failure under the insulation criterion of ASTM E119[1]. For the side with the single layer, the temperature rise was significant. The insulation failure criterion[1] was reached at 900 s after ignition. Based upon the total heat flux and exposed face temperature measurements, it is not surprising that the temperature at location 5 rose the quickest. Similar to Assembly One, differences in the maximum temperatures measured on the unexposed surface were observed.

9. Similar to Assembly One, the timeline of events from the video-graphic records agreed with the magnitude of the unexposed face temperature measurements. Locations where the most severe flaming was observed (5, 7, and 11) produced the highest measured temperature. The lower portion of section 1, near thermocouple location 12, produced the lowest temperatures since flaming was not observed at this location.

It is of value to compare the measurements obtained here with other published data; however, to authors' knowledge, no data exist for partition assembly behavior under actual fire conditions. Rather, most data have been obtained in test furnaces. Accordingly, the measurements under these fire exposures were compared to those.

- Heat flux: Sultan *et al.*[19] have performed heat flux measurements in a large-scale furnace designed to test walls and floors. In these experiments, two total heat flux gauges were mounted into a partition assembly and the assembly was subjected to the furnace exposure. Based on their findings, the total heat flux measured was nearly identical (within 2 %) at the two gauge locations. The total heat flux reached a value of 150 kW/m^2 in 6000 s. The furnace was operated up to 7200 s, where a maximum total heat flux of 170 kW/m^2 was measured.

These results are very different from those obtained in the current fire tests. The present measurements show the total heat flux varied with height, while in furnaces, the heat flux is uniform. In addition, the rate of increase of total heat flux measured in the furnace was considerably slower than the rates here. For example, in figure 7 (b), the total heat flux reached 100 kW/m^2 in 700 s. In the furnace, this did not occur until 2400 s. This shows that the amount of energy incident on the partition can occur much more quickly in an actual fire. Experiments with very different room fires by Fang[20] also showed this faster rise.

- Temperatures: Sultan[10] performed large-scale furnace tests for non-load bearing steel stud wall assemblies with the similar stud spacing (600 mm) and similar stud width (92 mm) as the present assemblies. The overall size was slightly larger than the assemblies reported here (3.05 m by 3.66 m). He made thermocouple measurements inside the cavity at similar locations to Assembly Two. In addition, unexposed face temperature measurements under insulating pads were also reported. He reported average temperatures at various locations and ran the test up to the time of insulation failure[1], which occurred at 3900 s. The most dramatic difference between the measurements of Sultan[10] and those of Assembly Two are the rate of temperature rise, both inside the cavity and on the outside face of unexposed board. Although Assembly Two did not reach insulation failure, the rate of temperature rise both inside the cavity and on the outside face of unexposed board was faster than the assembly subjected to the furnace test. Such information further confirms, based on the fire exposure data reported here, that the heating process inside the standard furnace can be much slower than actual fire conditions.

CONCLUSIONS

The detailed photographic measurements, in concert with heat flux and temperature measurements, have generated data for structural failure models. A complementary modeling effort[21] is using the collected data for model validation.

AKNOWLEDGEMENTS

The authors are indebted to the staff of the Large Fire Laboratory (LFL) at NIST for assistance in the experiments. Dr. Thomas Ohlemiller of BRFL-NIST is acknowledged for his guidance in performing total heat flux measurements.

REFERENCES

1. Test Method for Fire Resistance Tests of Building Construction and Materials, ASTM E119-00a, American Society for Testing and Materials.
2. Fire Resistance Tests – Elements of Building Construction, ISO 834 Parts 1 through 9, International Organization for Standardization, Geneva Switzerland.
3. R.W. Bukowski, Prediction of the Structural Fire Performance of Buildings, *8th Fire and Materials Conference*, San Francisco, CA (2003).
4. N.R. Keltner, J.L. Moya, Defining the Thermal Environment in Fire Tests, *Fire and Materials*, 14:133-138 (1989).
5. W.L. Grosshandler (Editor), Fire Resistance Determination and Performance Prediction Research Needs Workshop: Proceedings, *NISTIR 6890* (2002).
6. CIB-W14, Rational Fire Safety Engineering Approach to Fire Resistance of Buildings, Publication 269 (2001).

7. H. Takeda, A Model to Predict the Fire Resistance if Non-Load Bearing Wood-Stud Walls, *Fire and Materials*, 27:19-39 (2003).

8. H. Takeda, J.R. Mehaffey, Wall2D: A Model for Predicting Heat Trasfer through Wood-Stud Walls Exposed to Fire, *Fire and Materials*, 22:133-140 (1998).

9. L.R. Richardson, M. Batista, Revisiting the Component Additive Method for Light-Frame Walls Protected by Gypsum Board, *Fire and Materials*, 21:107-114 (1997).

10. M.A. Sultan, A Model for Predicting Heat Transfer Through Noninsulated Unloaded Steel-Stud Gypsum Board Wall Assemblies Exposed to Fire, *Fire Technology*, 32:239-259 (1996).

11. O. Axenenko, G. Thorpe, The modeling of dehydration and Stress Analysis of Gypsum Plasterboards Exposed To Fire, *Comp. Mat. Sci*. 6:281-294 (1996).

12. J.R. Mehaffey, P. Cuerrier, G. Carisse, A Model for Predicting Heat Transfer through Gpysum-Board/Wood-Stud Walls Exposed to Fire, *Fire and Materials*, 18: 297-305 (1994).

13. B. Fredlund, Modeling of Heat Transfer and Mass Transfer in Wood Structures During Fire, *Fire Safety Journal*, 20:39 (1993).

14. Standard Specification for Installation of Steel Framing Members to Receive Screw-Attaced Gypsum Panel Products, ASTM C754-00, American Society for Testing and Materials.

15. Standard Specification for Application of Finishing of Gypsum Board, ASTM C840-03, American Society for Testing and Materials.

16. Standard Specification for Nonstructural Steel Framing Members, ASTM C654-00, American Society for Testing and Materials.

17. Standard Specification for Steel-Piercing Tapping Screws for the Application of Gypsum Panel Products or Metal Plaster Bases to Wood or Steel Studs, ASTM C1002-01, American Society for Testing and Materials.

18. May 2004 Progress Report on the Federal Building and Fire Safety Investigation of the World Trade Center Disaster, Appendix J, "Interim Report on Experiments to Support Fire Dynamics and Thermal Response Modeling," *NIST Special Publication 1000-5*, in press.

19. M.A. Sultan, N. Benichou, B.Y. Min, Heat Exposure in Fire Resistance Furnaces: Full-Scale vs. Intermediate-Scale, *8th Fire and Materials Conference*, San Francisco, CA (2003).

20. J.P. Fang, Fire Development in Residential Basement Rooms, *NBSIR 80-2120* (1980).

21. S. Kukuck, K. Prasad, Heat and Mass Transfer Through Gypsum Partitions Subjected to Fire Exposure, *Structures in Fire Meeting*, Ottawa (2004).

FIGURE CAPTIONS

Fig. 1 (a) Drawing of Assembly One showing the location of the unexposed and exposed face temperature measurements. The location of the exposed face temperature measurements is the same for Assembly One and Assembly Two.

Fig. 2 (a) Drawing of Assembly Two, showing the location of the unexposed face temperature measurements. (b) Schematic of Assembly Two, showing the location of the interior temperature measurements.

Fig. 3 Drawing of partition construction at the exposed face. The location of the total heat flux gauges is the same for Assembly One and Assembly Two.

Fig. 4 (a) Temporal evolution of the exposed face temperature measurements for Assembly One as a function of location. (b) Temporal evolution of the total heat flux measurements for Assembly One as a function of location.

Fig. 5 (a) Temporal evolution of the exposed face temperature measurements for Assembly Two as a function of location. (b) Temporal evolution of the total heat flux measurements for Assembly Two as a function of location.

Fig. 6 (a) Temporal evolution of temperatures measured on the inside of the exposed face as a function of location. (b) Temporal evolution of temperatures measured on the inside of the unexposed face as a function of location.

Fig. 7 Temporal evolution of the unexposed face temperature measurements for Assembly Two as a function of location.

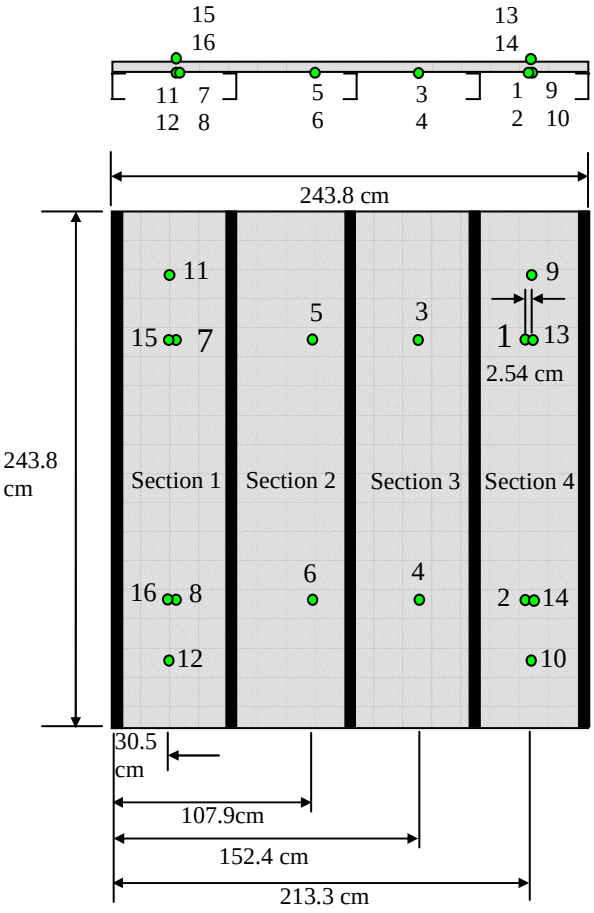

Fig. 1 (a)

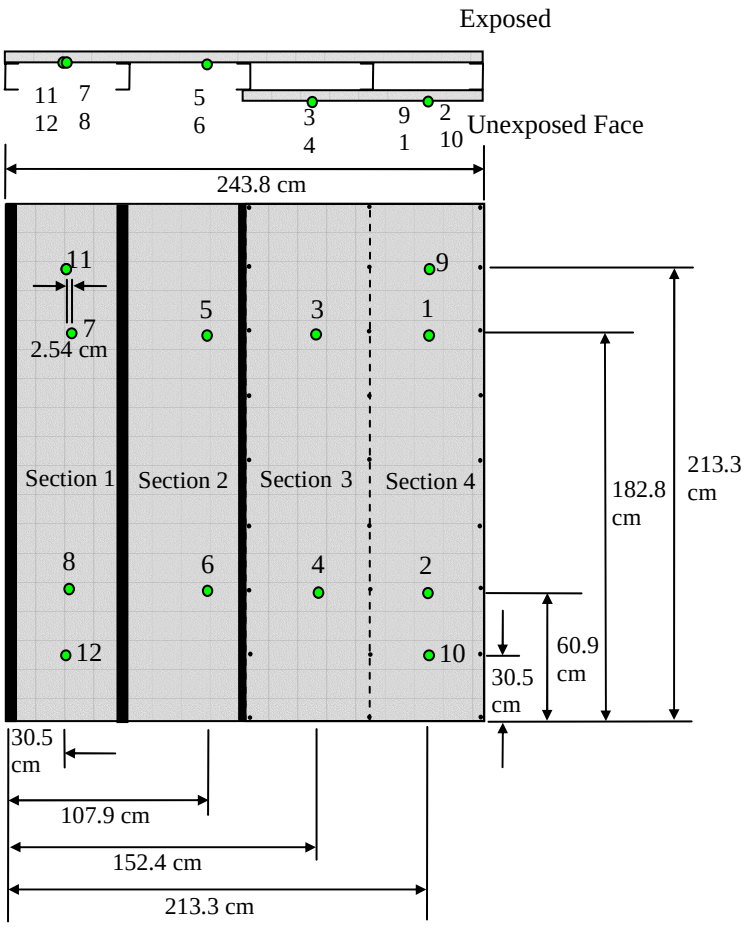

Fig. 2 (a)

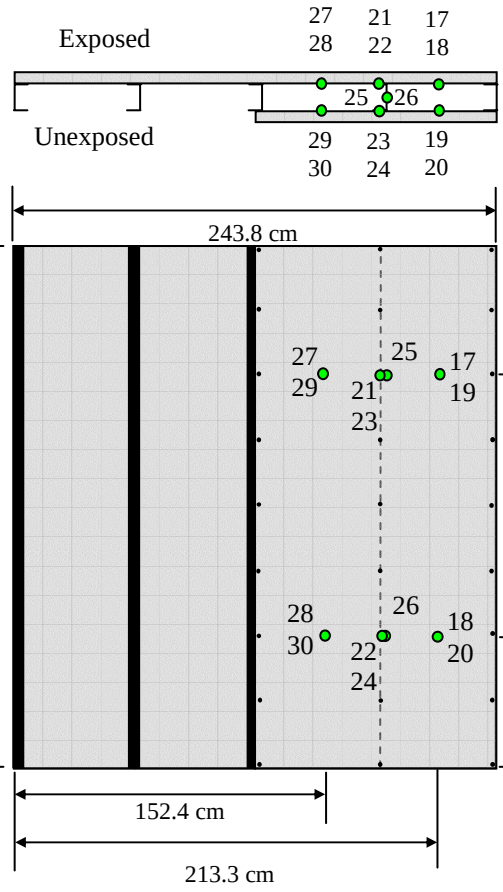

Fig. 2 (b)

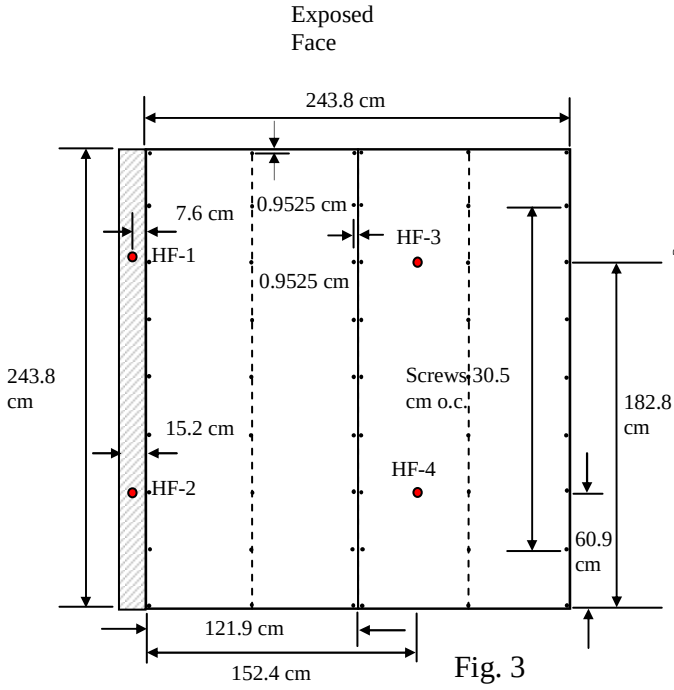
Exposed
Face
243.8 cm
7.6 cm
0.9525 cm
HF-1
HF-3
0.9525 cm
243.8
cm
Screws 30.5
cm o.c.
182.8
cm
15.2 cm
HF-4
HF-2
60.9
cm
121.9 cm
152.4 cm

Fig. 3

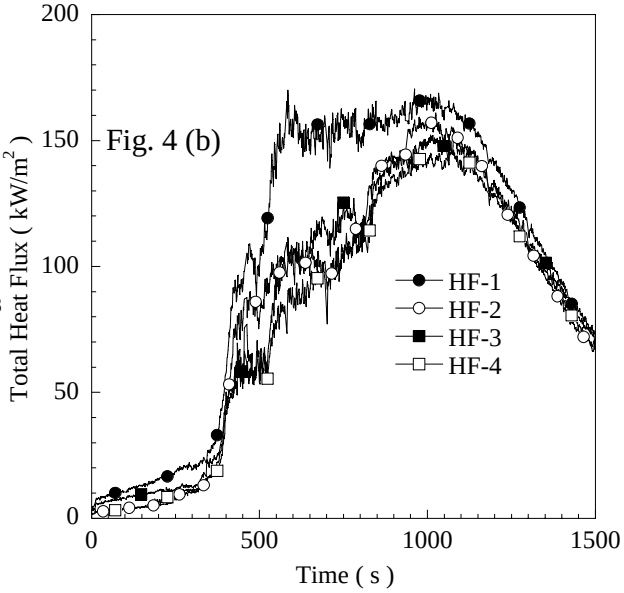
Fig. 4 (b)
Total Heat Flux (kW/m2)
Time (s)
HF-1
HF-2
HF-3
HF-4

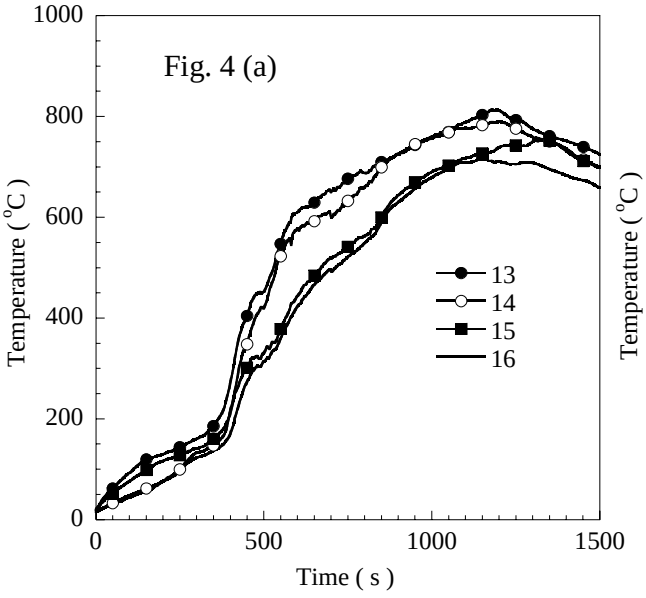
Fig. 4 (a)
Temperature (oC)
Time (s)
13
14
15
16

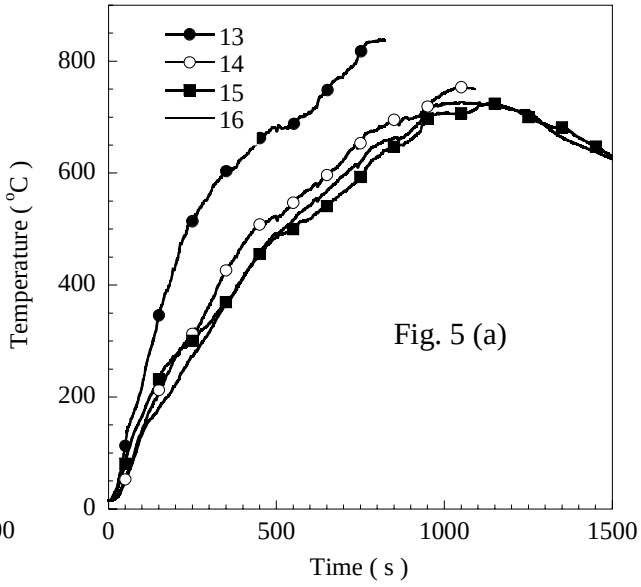
Fig. 5 (a)
Temperature (oC)
Time (s)
13
14
15
16

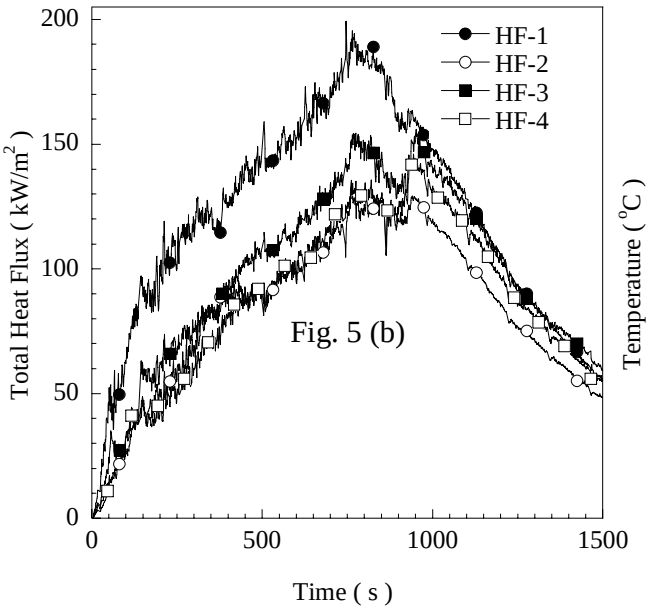
HF-1
HF-2
HF-3
HF-4
Fig. 5 (b)
Total Heat Flux (kW/m^2)
Time (s)

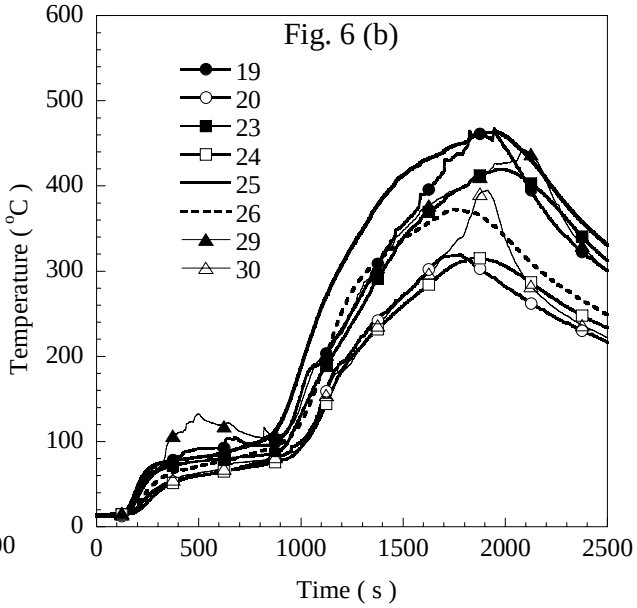
Fig. 6 (b)
19
20
23
24
25
26
29
30
Temperature (^{o}C)
Time (s)

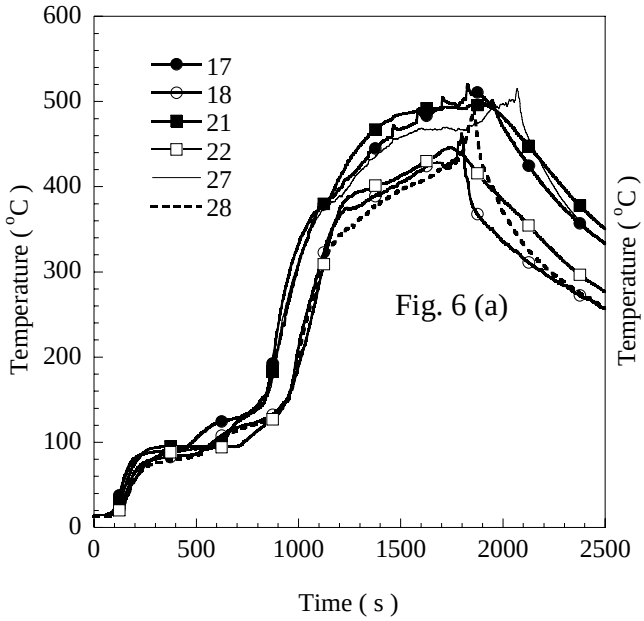
17
18
21
22
27
28
Fig. 6 (a)
Temperature (^{o}C)
Time (s)

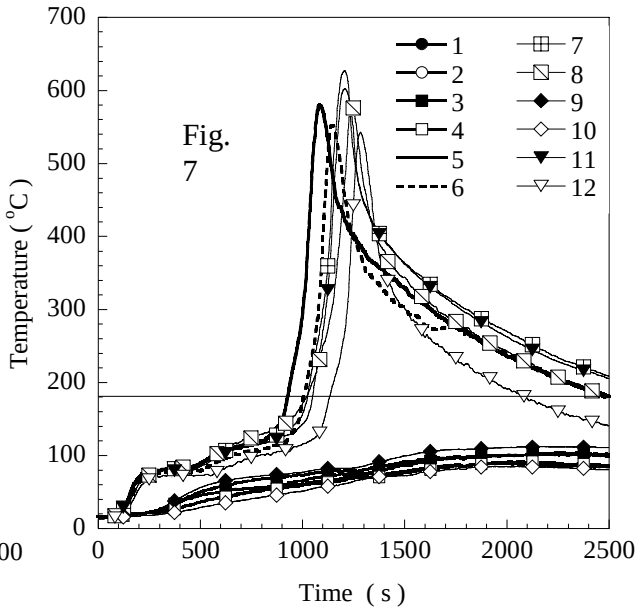
Fig. 7
1
2
3
4
5
6
7
8
9
10
11
12
Temperature (^{o}C)
Time (s)